

PAPER • OPEN ACCESS

Oxidative stress markers are elevated in exhaled breath condensate of workers exposed to nanoparticles during iron oxide pigment production

To cite this article: Daniela Pelclova *et al* 2016 *J. Breath Res.* **10** 016004

View the [article online](#) for updates and enhancements.

You may also like

- [Early-life oxidative stress due to air pollution. A scoping review focusing on identifying potential 'OMICS' biomarkers from body fluids](#)
J V F Coumans and S Al Jaaidi
- [Exhaled breath condensate \(EBC\) biomarkers in pulmonary fibrosis](#)
Sharron Chow, Paul S Thomas, Monique Malouf *et al.*
- [Concentration of exhaled breath condensate biomarkers after fractionated collection based on exhaled CO₂ signal](#)
Matteo Goldoni, Massimo Corradi, Paola Mozzoni *et al.*



The banner features a dark blue background with a molecular structure pattern in the top right corner. On the left, a tablet displays the book cover for 'The Breath Biopsy® Guide' (Fourth edition). A white starburst graphic with the word 'FREE' is positioned next to the tablet. The main title 'The Breath Biopsy® Guide' is written in large white font, with 'Fourth edition' in a smaller blue font below it. At the bottom, there is a blue button with the text 'DOWNLOAD THE FREE E-BOOK', an orange button with 'BREATH BIOPSY', and the Owlstone Medical logo.

The Breath Biopsy® Guide
Fourth edition

DOWNLOAD THE FREE E-BOOK

BREATH BIOPSY

OWLSTONE MEDICAL



PAPER

OPEN ACCESS

RECEIVED
29 August 2015

REVISED
5 December 2015

ACCEPTED FOR PUBLICATION
14 December 2015

PUBLISHED
1 February 2016

MADE OPEN ACCESS
1 March 2016

Original content from
this work may be used
under the terms of the
Creative Commons
Attribution 3.0 licence.

Any further distribution
of this work must
maintain attribution
to the author(s) and the
title of the work, journal
citation and DOI.



Oxidative stress markers are elevated in exhaled breath condensate of workers exposed to nanoparticles during iron oxide pigment production

Daniela Pelclova¹, Vladimír Zdimal², Petr Kacer³, Zdenka Fenclova¹, Stepanka Vlckova¹, Kamila Syslova³, Tomas Navratil⁴, Jaroslav Schwarz², Nadezda Zikova², Hana Barosova⁵, Francesco Turci⁶, Martin Komarc^{7,8}, Tomas Pelcl⁹, Jaroslav Belacek⁷, Jana Kukutschova⁵ and Sergey Zakharov¹

¹ Charles University in Prague and General University Hospital in Prague, First Faculty of Medicine, Department of Occupational Medicine, Na Bojišti 1, 128 00 Prague 2, Czech Republic

² Institute of Chemical Process Fundamentals of the AS CR, v.v.i., Rozvojová 1/135, 165 02 Prague 6, Czech Republic

³ Institute of Chemical Technology, Technická 5, 166 28 Prague 6, Czech Republic

⁴ J. Heyrovský Institute of Physical Chemistry of the AS CR, v.v.i., Dolejškova 3, 182 23 Prague 8, Czech Republic

⁵ Nanotechnology Centre, VSB—Technical University of Ostrava, 17. Listopadu 15, 708 33 Ostrava, Czech Republic

⁶ Interdepartmental Centre 'G. Scansetti' for Studies on Asbestos and Other Toxic Particulates and NIS Interdepartmental Centre for Nanostructured Interfaces and Surfaces, University of Torino, Via P. Giuria 7, I-10125 Torino, Italy

⁷ Charles University in Prague and General University Hospital in Prague, First Faculty of Medicine, Institute of Biophysics and Informatics, Salmovská 1, 120 00 Prague 2, Czech Republic

⁸ Charles University in Prague and General University Hospital in Prague, First Faculty of Medicine, Faculty of Physical Education and Sport, José Martího 31, 162 52 Prague 6, Czech Republic

⁹ Charles University in Prague and General University Hospital in Prague, First Faculty of Medicine, 3rd Medical Department, U Nemocnice 1, 128 08 Praha 2, Czech Republic

E-mail: daniela.pelclova@lfl.cuni.cz

Keywords: nanoparticles, Fe₂O₃, Fe₃O₄, exhaled breath condensate, urine, oxidative stress, occupational exposure

Abstract

Markers of oxidative stress and inflammation were analysed in the exhaled breath condensate (EBC) and urine samples of 14 workers (mean age 43 ± 7 years) exposed to iron oxide aerosol for an average of 10 ± 4 years and 14 controls (mean age 39 ± 4 years) by liquid chromatography-electrospray ionization-mass spectrometry/mass spectrometry (LC-ESI-MS/MS) after solid-phase extraction. Aerosol exposure in the workplace was measured by particle size spectrometers, a scanning mobility particle sizer (SMPS) and an aerodynamic particle sizer (APS), and by aerosol concentration monitors, P-TRAK and DustTRAK DRX.

Total aerosol concentrations in workplace locations varied greatly in both time and space. The median mass concentration was 0.083 mg m^{-3} (IQR $0.063\text{--}0.133 \text{ mg m}^{-3}$) and the median particle concentration was $66\,800 \text{ particles cm}^{-3}$ (IQR $16\,900\text{--}86\,900 \text{ particles cm}^{-3}$). In addition, more than 80% of particles were smaller than 100 nm in diameter.

Markers of oxidative stress, malondialdehyde (MDA), 4-hydroxy-trans-hexenal (HHE), 4-hydroxy-trans-nonanal (HNE), 8-isoProstaglandin F₂ α (8-isoprostane) and aldehydes C₆–C₁₂, in addition to markers of nucleic acid oxidation, including 8-hydroxy-2-deoxyguanosine (8-OHdG), 8-hydroxyguanosine (8-OHG), 5-hydroxymethyl uracil (5-OHMeU), and of proteins, such as o-tyrosine (o-Tyr), 3-chlorotyrosine (3-ClTyr), and 3-nitrotyrosine (3-NOTyr) were analysed in EBC and urine by LC-ESI-MS/MS.

Almost all markers of lipid, nucleic acid and protein oxidation were elevated in the EBC of workers comparing with control subjects. Elevated markers were MDA, HNE, HHE, C₆–C₁₀, 8-isoprostane, 8-OHdG, 8-OHG, 5-OHMeU, 3-ClTyr, 3-NOTyr, o-Tyr (all $p < 0.001$), and C₁₁ ($p < 0.05$). Only aldehyde C₁₂ and the pH of samples did not differ between groups. Markers in urine were not elevated.

These findings suggest the adverse effects of nano iron oxide aerosol exposure and support the utility of oxidative stress biomarkers in EBC. The analysis of urine oxidative stress biomarkers does not support the presence of systemic oxidative stress in iron oxide pigment production workers.

Abbreviations

3-ClTyr	3-chlorotyrosine
3-NOTy	3-nitrotyrosine
5-OHMeU	5-hydroxymethyl uracil
8-isoprostane	8-isoProstaglandine F2 α
8-OHdG	8-hydroxy-2'-deoxyguanosine
8-oxodG	8-oxo-7,8-dihydro-2'-deoxyguanosine
8-OHG	8-hydroxyguanosine
APS	aerodynamic particle sizer
BMI	body mass index
DNA	deoxyribonucleic acid
EBC	exhaled breath condensate
HHE	4-hydroxy-trans-hexenale
HNE	4-hydroxy-trans-nonenale
IQR	interquartile range
LC-ESI-MS/MS	liquid chromatography—electrospray ionization—tandem spectrometry
MDA	malondialdehyde
NIOSH	National Institute for Occupational Safety and Health
NO _x	nitrogen oxides
OECD	Organisation for Economic Co-operation and Development
OSHA	Occupational Safety and Health Administration
o-Tyr	o-tyrosine
PEL	permissible exposure limit
PM	particulate matter
PSD	particle number size distribution
RNA	ribonucleic acid
ROS	reactive oxygen species
SMP	scanning mobility particle sizer
SPE	solid-phase extraction
TWA	time-weighted average concentration

1. Introduction

Iron nanoparticles belong to 13 priority nanomaterial groups identified by the organisation for economic co-operation and development (OECD) for evaluation of their safety [1]. There is very little information about potential risks of occupational exposure to engineered nanoparticles during production and processing; therefore this is a widely debated issue. Studies on the effect of occupational exposure to engineered iron oxide nanoparticles have yet to be published [2] and no biological exposure tests have been developed to monitor workers' exposure [3].

Similar to all nanoparticles, iron oxide nanoparticles are associated with unique physicochemical properties that facilitate their use in novel applications. On the other hand, nano-scale particles with large surface area and enhanced reactivity can more readily diffuse across biological membranes and through tissue barriers. Based on experimental data, humans exposed to engineered nanomaterials could have oxidative damage in their respiratory system and in other organs due to systemic effects [3, 4].

Iron oxide nanoparticles, including Fe₂O₃ and Fe₃O₄, are found naturally in the environment during volcanic eruptions. In addition, they can be found in vehicle and industry emissions and air pollution particulates. They are also chemically synthesized for a wide variety of applications. For example, they are present in paint, ink, rubbers, plastics, cosmetics, and in medical devices [2].

Occupational exposure to iron oxides occurs during pigment production. These pigments have pure consistent properties and tinting strength. Ilmenite (FeTiO₃) is a steel-grey titanium-iron oxide mineral that is the source of iron oxides used in the pigment production industry. Red iron oxide pigments are produced by thermal decomposition in the process of roasting and calcination. α -Fe₂O₃ is obtained by oxidative calcination of decomposable iron compounds. The colour changes from red with a decreasing yellowish hue between 700–750 °C to red with an increasing bluish hue between 750–900 °C [5].

Single component forms are mainly produced as red (hematite, α -Fe₂O₃, 70% iron), yellow (limonite/goethite, FeO(OH), 63% iron) and black (magnetite, Fe₃O₄, 72% iron) pigment. A combination of Fe₂O₃ and Fe₃O₄ yields brown pigment [6]. These production processes generate high concentrations of small particles [7].

Nevertheless, the potential adverse health effects of iron oxide nanoparticles are poorly understood and limited information on the toxicological effects of these nanoparticles exists. However, it is now known that their toxicity may differ from that of their bulk counterparts. Experimental studies suggest that iron oxide nanoparticles can be distributed in secondary organs and induce damage in biological systems [8]. After inhalation, due to their small size, nanoparticles can deposit in the lower, gas exchange region of the lungs [9]. In addition, inhalation of iron oxide particles is more likely to have systemic effects, compared with ingestion and dermal exposure [2].

Nano-sized particles can directly interact with the plasma membrane and/or mitochondria NADPH oxidases, leading to disruption of the electron transport chain and generation of superoxide radicals [10]. According to Singh [11], iron oxide nanoparticles in cells can be degraded into Fe²⁺ in lysosomes. This 'free iron' has the potential to cross nuclear and mitochondrial membranes. In mitochondria, Fe²⁺ can react with hydrogen peroxide and oxygen to form highly reactive hydroxyl radicals and Fe³⁺ via the Fenton reaction. The generation of hydroxyl radicals and other reactive oxygen species (ROS) can result in lipid, protein and DNA damage, leading to impaired mitochondrial function, cellular stress, inflammation, cytotoxicity, apoptosis and genotoxicity [11, 12].

In rats, bronchoalveolar lavage and histopathology revealed decreased cell viability and lung injury following a single 4 h inhalation exposure to 640 mg m⁻³ iron oxide nanoparticles (Fe₃O₄, size 15–20 nm).

Within 24 h post-exposure, lung tissue malondialdehyde (MDA) concentration increased [13]. Inhalation of $\sim 20 \text{ mg m}^{-3}$ Fe_3O_4 aerosol for 4 h led to interstitial inflammation and macrophage infiltration in the alveolar region [9]. However, after a mild acute exposure to Fe_2O_3 , Sotiriou *et al* [14] found significantly elevated levels of ROS in the lungs and hearts of rats exposed for 5 h to $100\text{--}200 \text{ }\mu\text{g m}^{-3}$ Fe_2O_3 . Systemic effects, specifically hepatic and renal injury caused by oxidative stress, were observed after intraperitoneal injection of Fe_3O_4 nanoparticles in mice. This mechanism was supported by an increase in tissue MDA and 8-hydroxy-2'-deoxyguanosine (8-OHdG) at doses of 20 mg kg^{-1} of body weight [15]. After intravenous injection of $\gamma\text{-Fe}_2\text{O}_3$ (0.8 mg kg^{-1}) in rats, inflammation in the lungs, liver and kidneys suggested small particles crossed endothelial barriers related to vascularisation and vessel permeability in these organs [4]. Similarly, in experimental studies on human cells, oxidative stress markers were elevated in lung bronchial cells, fibroblasts [10, 16], endothelial cells [4], and bone marrow mesenchymal stromal cells [17] following exposure to iron oxide nanoparticles.

In humans, markers of oxidative stress, MDA, 4-hydroxy-trans-hexenal (HHE), HNE, 8-isoProstaglandin $\text{F}_{2\alpha}$ (8-isoprostane) and aldehydes $\text{C}_6\text{--}\text{C}_{12}$ are used to detect lipid oxidation [18]. Nitrotyrosine (3-NOTyr) is a marker for nitration stress, 3-chlorotyrosine (3-ClTyr) is a specific molecular marker for the production of chlorinating oxidants by eosinophil peroxidase and myeloperoxidase systems in leukocytes, and o-tyrosine (o-Tyr) is an amino acid oxidation biomarker. In nuclear DNA, 8-OHdG, i.e. 8-oxo-7,8-dihydro-2'-deoxyguanosine (8-oxodG), is the predominant form of free radical-induced oxidative lesions, similar to 8-hydroxyguanosine (8-OHG) and hydroxymethyl uracil (5-OHMeU) in RNA. Therefore, several markers of oxidative stress have been widely used as biomarkers for oxidative stress and carcinogenesis, in particular lung carcinogenesis [19–21].

Besides occupational exposure, epidemiological studies have shown that environmental exposure to air pollution is associated with detrimental effects including disorders related to oxidative stress [22–24]. For example, MDA was suggested as a biomarker of oxidative stress in the respiratory tract in relation to air pollution exposure, and MDA and 8-OHdG were suggested as urine biomarkers for systemic oxidative stress [19, 25, 26].

Exhaled breath condensate (EBC) is a liquid that reflects the composition of the fluid lining the airway [27]. It is obtained non-invasively from subjects after cooling of exhaled air. EBC is composed mainly of water (99.9%) and a small proportion of water-soluble and insoluble compounds. These non-volatile compounds can include small inorganic ions, large organic molecules (urea, organic acids, amino acids), proteins and macromolecules that presumably originate from the airway lining fluid in the form of aerosolized particles [28]. The analysis of EBC allows the source of

biomarkers, originally formed in airways and lungs, to be tracked.

The aim of this study was to evaluate markers of oxidative stress in the EBC of workers exposed to iron oxide nanoparticles during iron oxide pigment production and their association with workplace environments.

2. Methods

2.1. Subjects

After work-shifts, EBC and urine samples were collected in 14 workers (males, 43 ± 7 years, 43% smokers). Their mean length of exposure to iron oxides was 10 ± 4 years. The control group was composed of 14 males (39 ± 4 years, 50% smokers), who were not employed in this factory and were not exposed occupationally to dust or other health risks (safety inspectors and office workers). Both groups were examined according to the following scheme: a physical examination, a standardized questionnaire with questions on personal and occupational history, treatments, dietary habits, smoking habits and alcohol intake.

EBC samples were collected using Ecoscreen Turbo (DECCS, Jaeger, Germany). All subjects breathed tidally for about 15 min through a mouthpiece connected to a condenser (-20°C) while wearing a nose-clip. A constant volume of exhaled air of 120 L was maintained using EcoVent device by Jaeger, Germany, and time of collection was about 15 min. All samples were immediately frozen and stored at -80°C .

2.1.1. Ethics

The study was conducted according to the Declaration of Helsinki. The Ethical Committee of the 1st Medical Faculty, Charles University approved the study.

2.2. Analysis of oxidative stress markers in EBC and urine

MDA, HNE, HHE, 8-isoprostane, aldehydes $\text{C}_6\text{--}\text{C}_{12}$, 8-OHdG, 8-OHG, 5-OHMeU, o-Tyr, 3-ClTyr and 3-NOTyr were analysed after solid-phase extraction (SPE) by liquid chromatography—electrospray ionization—tandem spectrometry (LC-ESI-MS/MS) using deuterium-labelled internal standards, as previously described [29, 30]. Conductivity was measured as a reference indicator in EBC dilution to take into account changes in respiratory solute concentration [31]. To exclude contamination of EBC by saliva, α -amylase concentration was determined [31]. In addition, pH has been measured [32]. Biomarker concentrations in urine samples were normalised to urinary creatinine concentration [33]. Furthermore, all samples were blinded to personnel involved in sample analysis.

2.3. Workplace aerosol measurements

Pilot measurements of total particle concentrations were determined to construct concentration maps,

localize main aerosol sources and determine locations of high iron oxide pigment. Total particle number and mass concentrations were mapped using P-Trak® Ultrafine Particle Counter 8525 (P-TRAK) (TSI Inc., Minneapolis, USA) and DustTrak™ DRX Aerosol Monitor 8533 (DustTrak) (TSI Inc., Minneapolis, USA), respectively.

For the 8-h shift samples, three locations were selected: (1) the calcination furnace, (2) drying units, and (3) the control room. These three locations were selected because workers frequently worked there. The aim of these measurements was to determine changes in particle size distribution during shifts to estimate workers' exposure to airborne particulates.

The instruments used were two aerosol size spectrometers, a Scanning Mobility Particle Sizer™ (SMPS) model 3936 L (TSI Inc., Minneapolis, USA), and an Aerodynamic Particle Sizer® Spectrometer (APS) model 3321 (TSI Inc., Minneapolis, USA). The aerosol spectrometers sampled synchronously with a 5 min time resolution, covering overall particle diameters from 15 nm–10 µm, and with a size resolution of 32 channels/decade. As the particle size distributions (PSDs), measured by SMPS and APS, overlapped in the size range of 0.5–1 µm, the total particle number and mass concentration determined as a sum of these two instruments had to be corrected for this overlap. Without this correction, the error in total concentration would have been 10–25% of total concentration, depending on the distribution shape.

At the beginning of the work-shift, the SMPS and APS were placed at one of the preselected locations, usually several meters away from manufacturing equipment and preferably at a location where workers walked by. After performing routine spectrometer checks, the SMPS and APS were left unattended while samples were continuously collected during 8-h shifts. For each shift, spectrometers were moved to different locations.

During measurements, random checks were performed to compare total particle number concentrations determined by SMPS and APS with P-TRAK values (the differences between averaged values never exceeded 20%). Similarly, PM₁₀ mass concentrations determined by DustTrak were compared with the PM₁₀ integrated from the combined SMPS and APS data (particle density was assumed to be 5.24 g cm⁻³). Workers spent the majority of their time in the control room with a closed door. The second most frequented area was near the calcination furnace, which emitted particles.

2.4. Raman spectra of dust sediment from the production process

Five samples of dust sediment on the workshop floor were collected from different stages of production, i.e. calcination, milling and drying during the production of different pigments (red, yellow and brown) and analysed by Raman microspectroscopy using the Smart Raman Microscopy System XploRATM

(HoribaYvonJobin, France). Raman spectra were acquired with a 532 nm excitation laser source and 1200 grooves mm⁻¹ grating. Multiple parts of the samples were chosen for further analysis.

2.5. Environmental air contamination

Air concentrations of SO₂, O₃, nitrogen oxides (NO_x), particulate matter (PM)_{2.5} and PM₁₀, recorded on hourly basis were taken on the same days workers were examined. The value related to the same hour when the post-shift and control EBC samples were obtained. Air concentrations were obtained from the National Hydrometeorological monitoring system at the closest stationary monitoring station. In the case of workers, the distance to the site of EBC collection was 1.6 km, and in controls the distance was 1.5 km. The following analytical methods were used: UV-fluorescence (SO₂), chemiluminescence (NO_x), UV-absorption (O₃), and an optoelectronic method (PM).

2.6. Statistics

Basic descriptive statistics (mean, median, confidence interval, standard deviation, skewness, and kurtosis) were computed for all variables, which were subsequently tested for normality using the Kolmogorov-Smirnov test. The chi-square test was used to compare frequency counts of demographic categorical variables (smoking, and alcohol consumption) in groups of workers versus controls. Differences in interval demographic variables were tested using independent-groups *t*-test (for normally distributed variables) and the Mann-Whitney *U* test (for non-normally distributed variables). The independent-groups *t*-test was used for workers versus controls. The bivariate relationship between variables under study was assessed using the Spearman correlation coefficient. Statistical significance was set at *p* < 0.05. Multiple regression analysis was used to predict markers of oxidative stress in EBC by a set of predictors (Fe exposure—yes/no, age, smoking—yes/no, alcohol consumption—yes/no, BMI, SO₂, NO_x, O₃). All analyses were conducted using SPSS version 22.0 (SPSS, Inc., Chicago, IL).

3. Results

3.1. Subjects

There were no differences in age, BMI, prevalence of smoking and alcohol consumption in the groups studied (all *p* > 0.05, data not shown).

3.2. Analysis of oxidative stress markers in EBC and urine

As shown in figures 1 and 2, almost all markers of oxidation of lipids, nucleic acids, and proteins in the EBC (MDA, HNE, HHE, C₆–C₁₀, 8-isoprostane, 8-OHdG, 8-OHG, 5-OHMeU, 3-ClTyr, 3-NOTyr, o-Tyr) were elevated (all *p* < 0.001), including C₁₁ (*p* < 0.05) in workers compared with control subjects.

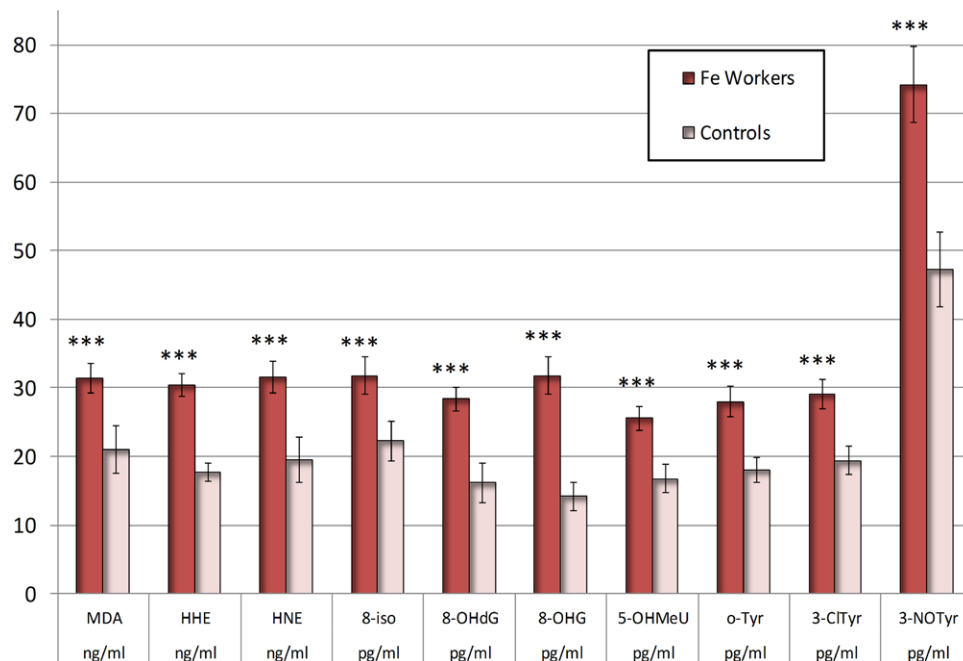


Figure 1. Malondialdehyde (MDA), 4-hydroxy-trans-hexenal (HHE), 4-hydroxy-trans-nonenal (HNE), 8-isoProstaglandin $F_{2\alpha}$ (8-isoprostane, 8-iso), 8-hydroxy-2-deoxyguanosine (8-OHdG), 8-hydroxyguanosine (8-OHG), hydroxymethyl uracil (5-OHMeU), o-tyrosine (o-Tyr), 3-chlorotyrosine (3-ClTyr), and nitrotyrosine (3-NOTyr) in the exhaled breath condensate (EBC) of iron oxide exposed workers and controls. The symbols *** denote the significance levels of data equivalency gained from the workers and controls ($p < 0.001$). The bars denote the confidence levels ($p = 0.05$).

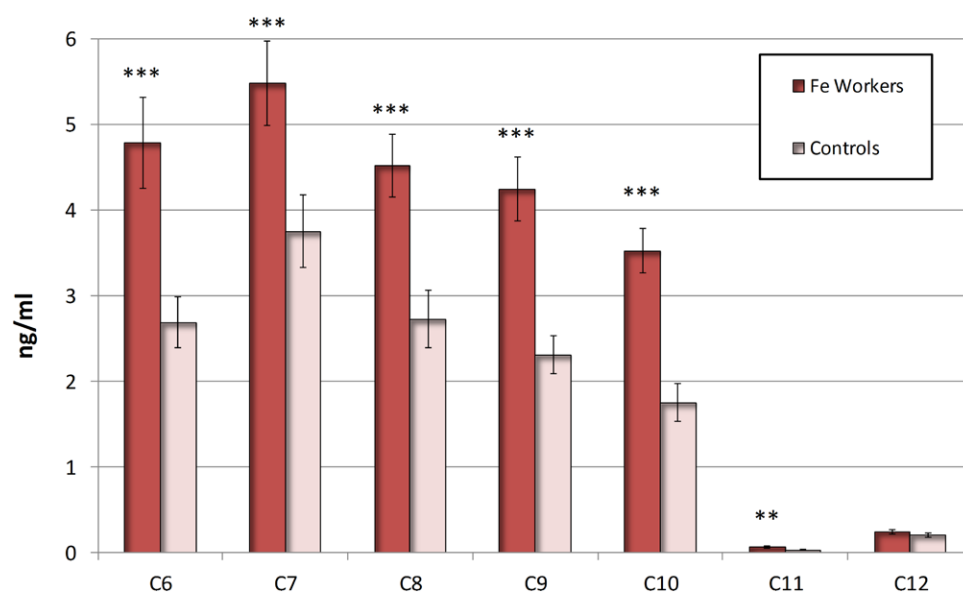


Figure 2. Aldehydes C_6 – C_{12} in the exhaled breath condensate (EBC) in iron oxides exposed workers and controls. The symbols ***, **, denote the significance levels of data equivalency gained from the workers and controls. *** ($p < 0.001$) ** ($p < 0.01$). The bars denote the confidence levels ($p = 0.05$).

Only aldehyde C_{12} was not increased. There was no difference in EBC conductivity and pH (5.40 ± 0.17 ; 5.30 ± 0.08) between workers and controls, respectively. There was no difference between the pH of the smokers and controls, either.

In workers, no positive correlation was found between EBC markers and age, lifestyle factors (smoking, alcohol intake) and presence of disease including rhinitis and chronic bronchitis. No correlation was

found between the presence of markers (both EBC and urine) and sample collection time.

On the other hand, markers of oxidative stress in urine were not significantly different in workers and controls. Slightly elevated levels of C_6 , C_7 and C_9 in workers did not reach statistical significance. However, correlations were observed between several EBC and urine markers of oxidative stress. Among them, MDA, C_6 and C_9 urine concentration correlated with EBC lev-

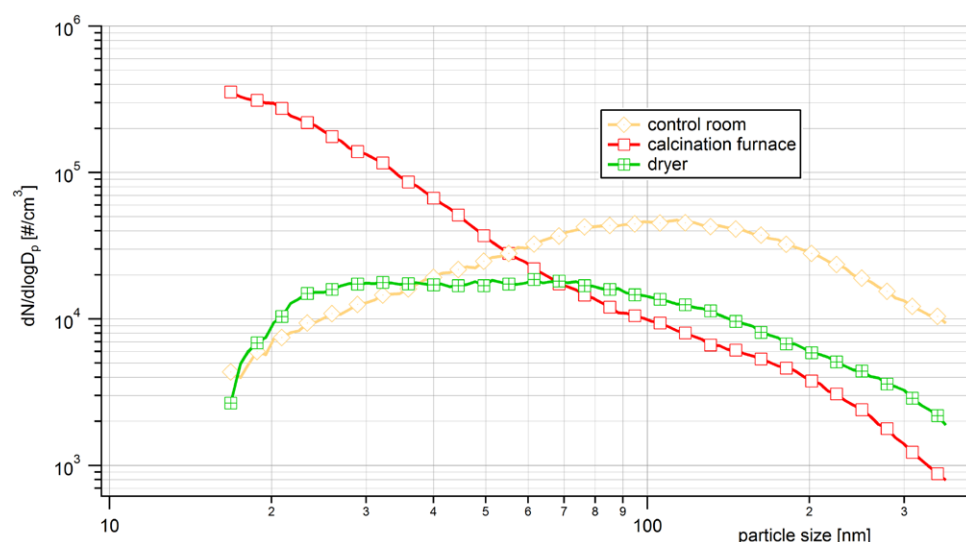


Figure 3. Median particle size distributions (PSD) in the control room, near the exit of the calcination furnace and near the dryer. Measurements were obtained by SMPS (14–350 nm) during three work-shifts.

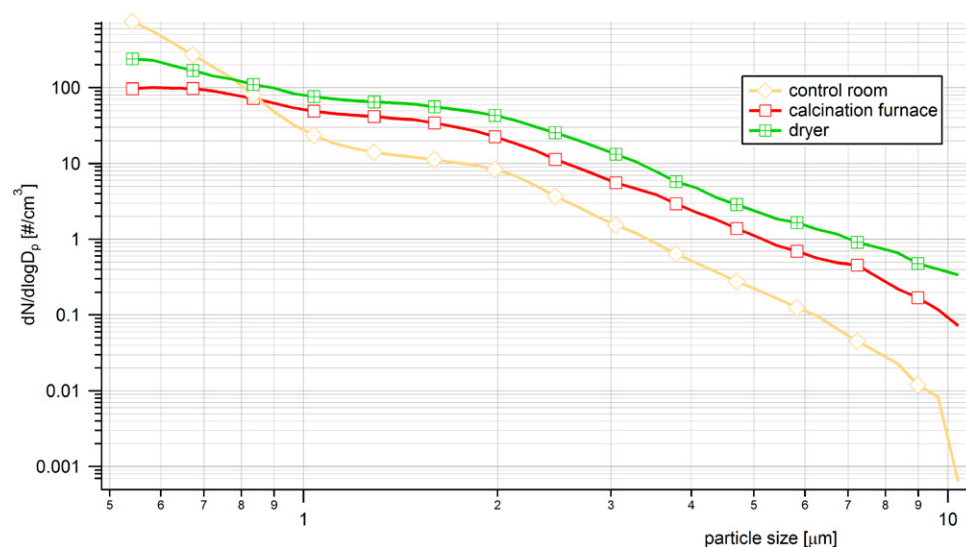


Figure 4. Median particle size distributions in the control room, near the exit of the calcination furnace, and near the dryer. Measurements were obtained by APS (0.5–10 μm) during three work-shifts.

els of the same markers. Additionally, C_6 in EBC correlated with HNE, C_7 – C_{10} , and OHdG in urine, and C_9 in EBC correlated with all other urine markers ($p < 0.05$).

3.3. Workplace aerosol measurements

Total workshop aerosol concentrations varied greatly in both time and space. Median mass concentration in the production unit of the plant was 0.083 mg m^{-3} (IQR 0.063 – 0.133 mg m^{-3}) and the particle number concentration was $66,800 \text{ particles cm}^{-3}$ (IQR $16,900$ – $86,900 \text{ particles cm}^{-3}$).

The mass concentration at the calcination furnace (0.069 mg m^{-3} (IQR 0.061 – 0.083 mg m^{-3})) was lower than that at the drying unit (0.136 mg m^{-3} (IQR 0.079 – 0.236 mg m^{-3})). However, the calcination furnace had a higher particle number concentration ($86,100 \text{ particles cm}^{-3}$ (IQR $80,000$ – $103,000 \text{ particles cm}^{-3}$)) than the

drying unit ($15,900 \text{ particles cm}^{-3}$ (IQR $13,000$ – $22,700 \text{ particles cm}^{-3}$)).

Surprisingly, the operating room had the highest mass concentration (0.243 mg m^{-3} (IQR 0.175 – 0.311 mg m^{-3})) but an average particle number concentration ($34,100 \text{ particles cm}^{-3}$ (IQR $25,900$ – $42,800 \text{ particles cm}^{-3}$)).

Median particle size distributions (during one work-shift) at each of the three locations (control room, calcination furnace and dryer) were measured by SMPS (figure 3) and APS (figure 4) spectrometers.

The highest particle number concentrations measured by SMPS (14–710 nm) were found near the calcination furnace, where the highest value $\sim 3 \times 10^5 \text{ particles cm}^{-3}$ was found at smallest detectable particle sizes. This suggests there were many particles smaller than 14 nm at this location. This corresponds

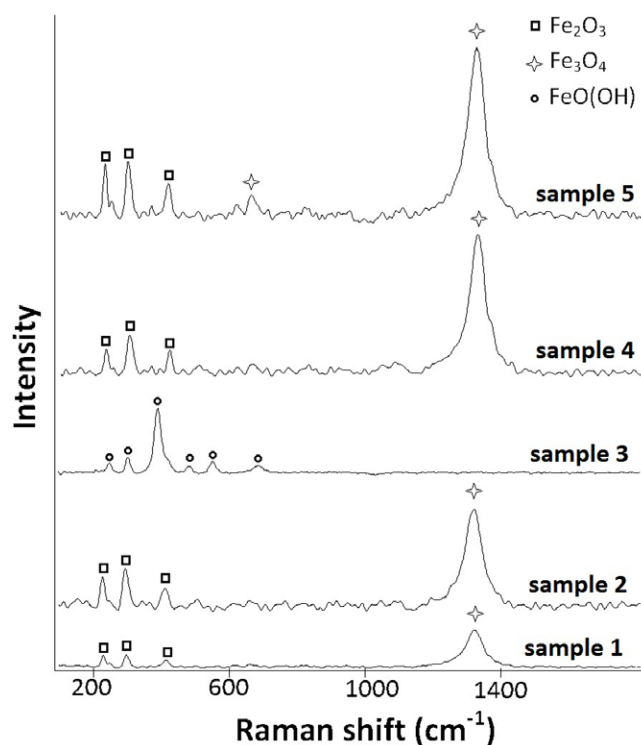


Figure 5. Raman spectra of dust sediment samples from the workplace. Red dust: samples 1, 2; yellow dust: sample 3; brown dust: sample 4; brown-red dust: sample 5.

to a gas-to-particle conversion process whereby gaseous precursors react to form less volatile reaction products that condense to form new particles. At the calcination furnace, particle number concentration decreased as particle size increased. The concentration of 55 nm particles at the calcination furnace was lower than in the control room and correspondingly, the concentration of particles >70 nm was lowest at the calcination furnace. Surprisingly, in the accumulation peak at ~ 100 nm, the highest particle number concentration ($\sim 5 \times 10^4$ particles cm^{-3}) was found in the control room. This indicates that there was a separate source of accumulation peak particles and these particles were not transferred to other parts of the production plant. We can only speculate about the nature of these particles. The lowest concentrations were found at the dryer with a maximum concentration of approximately 2×10^4 particles cm^{-3} . The PSD was broad and flat with two detectable peaks at 30 and 70 nm that likely reflected particles that were transported from other parts of the production plant; however these peaks were not much higher than of background (ambient air).

Median particle number size distributions determined by the APS spectrometer ($0.5\text{--}10\text{ }\mu\text{m}$) are shown in figure 4. All three PSD were decreased as particle size increased. The highest particle number concentrations were found at the dryer and were $\sim 2 \times$ higher than corresponding concentrations at the calcination furnace. The PSD with the steepest curve was from the control room and the smallest APS size was $\sim 2 \times$ higher than at the dryer. These particles likely came from the

same source as those from the upper size of the spectra measured by SMPS (figure 3). At the right end of the particle size axis in figure 4, control room PSD was more than an order of magnitude lower than at the dryer and in the calcination furnace area. The explanation for the much steeper decline of the PSD is simple: the surface to volume ratio of the control room was by far the highest of all three locations; therefore, the deposition of particles on surfaces was greatest.

It is worth noting that at any part of the plant, the medium dust concentration did not exceed the national allowed concentration of 10 mg m^{-3} for inert dust.

3.4. Raman spectra of dust sediment

Raman spectra of dust sediment samples are shown in figure 5. Raman spectra of samples 1, 2, 4 and 5 show the presence of $\alpha\text{-Fe}_2\text{O}_3$ with significant bands at 227 cm^{-1} , 298 cm^{-1} and 414 cm^{-1} and the presence of Fe_3O_4 with a significant band at 1322 cm^{-1} [34]. Samples 1 and 2 were found during red pigment production with a minor presence of Fe_3O_4 . The Raman spectrum of sample 3 collected during the production of yellow pigment, shows bands at 240 cm^{-1} , 296 cm^{-1} , 395 cm^{-1} , 476 cm^{-1} , 543 cm^{-1} and 678 cm^{-1} , consistent with the presence of FeO(OH) [34]. Raman spectra of samples 4 and 5 show a mixture of $\alpha\text{-Fe}_2\text{O}_3$ and Fe_3O_4 , consistent with brown pigment components.

3.5. Environmental air contamination

The level of air pollution with SO_2 , NO_x , O_3 , $\text{PM}_{2.5}$ and PM_{10} at both sites was classified by the National

Table 1. Multiple regression analysis (regression coefficient and 95% CI) of Fe oxides exposure, age, smoking, alcohol, body mass index (BMI), environmental air contamination and markers of oxidation of lipids, malondialdehyde (MDA), 4-hydroxy-trans-hexenal (HHE), 4-hydroxy-trans-nonanal (HNE), 8-isoProstaglandin F_{2α} (8-isoprostane, 8-iso) in the exhaled breath condensate.

	MDA	HHE	HNE	8-isoprostane
Fe exposure (Yes/No)	10.05 ^b (3.36, 16.74)	14.58 ^c (10.65, 18.50)	7.91 ^a (1.48, 14.34)	10.16 ^b (4.68, 15.65)
Age (years)	−0.11 (−0.34, 0.11)	−0.04 (−0.17, 0.10)	−0.01 (−0.23, 0.20)	0.14 (−0.05, 0.32)
Smoking (Yes/No)	1.36 (−3.46, 6.19)	1.11 (−1.72, 3.94)	−3.52 (−8.16, 1.11)	−2.24 (−6.20, 1.72)
Alcohol (Yes/No)	−1.91 (−13.07, 9.26)	1.69 (−4.86, 8.25)	0.80 (−9.93, 11.52)	−1.42 (−10.58, 7.74)
BMI (kg m ^{−2})	−0.08 (−0.63, 0.48)	−0.23 (−0.55, 0.10)	0.04 (−0.49, −0.57)	0.19 (−0.27, 0.64)
SO ₂ (μg m ^{−3})	0.02 (−0.10, 0.14)	0.00 (−0.07, 0.07)	0.03 (−0.09, 0.14)	−0.13 ^a (−0.23, −0.03)
NO _x (μg m ^{−3})	−0.01 (−0.08, 0.06)	0.01 (−0.03, 0.06)	−0.05 (−0.12, 0.02)	0.00 (−0.06, 0.06)
O ₃ (μg m ^{−3})	−0.14 (−0.01, 0.28)	−0.03 (−0.12, 0.05)	0.15 ^a (0.01, 0.29)	0.17 ^b (0.06, 0.29)

^a ($p < 0.05$),^b ($p < 0.01$), and^c ($p < 0.001$).**Table 2.** Multiple regression analysis (regression coefficient and 95% CI) of Fe oxides exposure, age, smoking, alcohol, BMI and environmental air contamination and aldehydes C₆–C₁₁ in the exhaled breath condensate.

	C ₆	C ₇	C ₈	C ₉	C ₁₀	C ₁₁
Fe exposure (Yes/No)	2.75 ^c (1.94, 3.56)	1.47 ^a (0.21, 2.72)	2.15 ^c (1.37, 2.93)	2.50 ^c (1.94, 3.06)	1.96 ^c (1.33, 2.59)	0.04 ^b (0.02, 0.07)
Age (years)	0.01 (−0.01, 0.04)	0.00 (−0.05, 0.04)	−0.01 (−0.04, 0.01)	0.01 (0.00, 0.03)	0.00 (−0.02, 0.02)	0.00 (0.00, 0.00)
Smoking (Yes/No)	−0.36 (−0.94, 0.23)	−0.01 (−0.92, 0.89)	0.13 (−0.43, 0.69)	−0.10 (−0.50, 0.31)	−0.01 (−0.47, 0.44)	−0.01 (−0.02, −0.01)
Alcohol (Yes/No)	−0.66 (−2.01, 0.69)	0.88 (−1.21, 2.97)	0.38 (−0.93, 1.68)	0.21 (−0.72, 1.14)	−0.07 (−1.12, 0.97)	0.01 (−0.03, 0.06)
BMI (kg m ^{−2})	−0.06 (−0.12, 0.01)	0.01 (−0.09, 0.11)	0.00 (−0.07, 0.06)	−0.03 (−0.07, 0.02)	−0.01 (−0.06, 0.04)	0.00 (0.00, 0.00)
SO ₂ (μg m ^{−3})	−0.03 ^b (−0.04, −0.01)	0.01 (−0.02, 0.03)	−0.02 ^a (−0.03, 0.00)	−0.02 ^c (−0.03, −0.01)	−0.01 (−0.02, 0.00)	0.00 (0.00, 0.00)
NO _x (μg m ^{−3})	0.00 (−0.01, 0.01)	0.00 (−0.01, 0.01)	0.00 (−0.01, 0.01)	0.00 (0.00, 0.01)	0.00 (−0.01, 0.01)	0.00 (0.00, 0.00)
O ₃ (μg m ^{−3})	0.00 (−0.02, 0.01)	0.01 (−0.02, 0.03)	0.01 (−0.01, 0.02)	0.00 (−0.01, 0.01)	0.00 (−0.01, 0.01)	0.00 (0.00, 0.00)

^a ($p < 0.05$),^b ($p < 0.01$), and^c ($p < 0.001$).

Hydrometeorological monitoring system as very low or low (data not shown). No values exceeded the recommended limits.

3.6. Association of EBC markers with occupational exposure

The multiple regression analysis confirmed a significant association between occupational exposure

and the concentration of all markers of oxidative stress in EBC, as shown in tables 1–3. Age, BMI, lifestyle and environmental parameters were not positively associated, with the exception of O₃ with HNE and 8-isoprostane. Surprisingly, some markers of environmental pollution were negatively correlated with EBC markers, for example with SO₂ with 8-isoprostane, C₆, C₈, C₉ and 8-OHG.

Table 3. Multiple regression analysis (regression coefficient and 95% CI) of Fe oxides exposure, age, smoking, alcohol, BMI and environmental air contamination and markers of oxidation of nucleic acids and proteins, 8-hydroxy-2-deoxyguanosine (8-OHdG), 8-hydroxyguanosine (8-OHG), hydroxymethyl uracil (5-OHMeU), o-tyrosine (o-Tyr), 3-chlorotyrosine (3-ClTyr), and nitrotyrosine (3-NO₂Tyr) in the exhaled breath condensate.

	8-OHdG	8-OHG	5-OHMeU	o-Tyr	3-ClTyr	3-NO ₂ Tyr
Fe exposure (Yes/No)	12.20 ^b (6.00, 18.40)	20.93 ^b (15.91, 25.94)	9.94 ^b (5.61, 14.28)	7.98 ^a (2.84, 13.12)	12.70 ^b (7.53, 17.87)	29.78 ^b (16.46, 43.10)
Age (years)	0.05 (−0.15, 0.26)	0.02 (−0.14, 0.19)	0.06 (−0.09, 0.20)	0.09 (−0.08, 0.27)	0.04 (−0.14, 0.21)	0.03 (−0.42, 0.48)
Smoking (Yes/No)	0.30 (−4.18, 4.77)	0.10 (−3.52, 3.71)	−0.77 (−3.90, 2.36)	−1.47 (−5.18, 2.24)	−1.79 (−5.52, 1.93)	1.18 (−8.43, 10.79)
Alcohol (Yes/No)	4.95 (−5.40, 15.30)	−3.26 (−11.63, 5.11)	−3.86 (−11.10, 3.38)	−2.52 (−11.11, 6.06)	0.68 (−7.95, 9.30)	0.36 (−21.88, 22.59)
BMI (kg m ^{−2})	−0.27 (−0.79, 0.24)	0.02 (−0.39, 0.44)	−0.03 (−0.39, 0.33)	−0.11 (−0.54, 0.31)	−0.26 (−0.68, −0.17)	−0.81 (−1.91, −0.29)
SO ₂ (μg m ^{−3})	0.01 (−0.10, 0.12)	−0.16 ^a (−0.25, −0.07)	−0.08 (−0.15, 0.00)	0.00 (−0.10, −0.09)	−0.05 (−0.15, 0.04)	−0.14 (−0.38, 0.10)
NO _x (μg m ^{−3})	0.00 (−0.07, 0.06)	0.00 (−0.06, 0.05)	−0.01 (−0.06, 0.03)	−0.04 (−0.09, 0.02)	0.02 (−0.03, 0.08)	−0.06 (−0.20, 0.09)
O ₃ (μg m ^{−3})	0.01 (−0.13, 0.14)	−0.06 (−0.16, 0.05)	−0.08 (−0.17, 0.01)	0.07 (−0.04, 0.18)	−0.05 (−0.16, 0.06)	−0.04 (−0.33, 0.25)

^a ($p < 0.01$), and

^b ($p < 0.001$).

4. Discussion

To the best of our knowledge, this study examining oxidative stress markers in iron oxide workers exposed to nanoparticles is the first of its kind in the occupational medicine field. Although workers did not complain of any symptoms, the presence of oxidative stress markers in the EBC of workers compared with controls shows a biological effect of nanoparticle exposure.

In a recent review, Lewinski *et al* [2] analysed results from both occupational exposure studies and controlled human volunteer inhalation studies. However, no occupational study focused on nanoparticle exposure. Additionally, these studies had poorly defined criteria for iron oxide aerosol exposure. In the volunteer studies, Fe₂O₃ or Fe₃O₄ iron oxide particles with diameters ranging from 1–6 μm were used. Volunteer inhalational studies confirmed two phases of clearance: a fast phase (several days) representing mucociliary clearance in the tracheobronchial tree, and a slow phase (several years) representing macrophage clearance in the alveolar region. This is in agreement with the slow disappearance (reduction in size and profusion) of x-ray opacities in welders due to the recovery of retained iron oxide particles. Welding fumes are classified as possibly carcinogenic for humans (group 2B) by the International for Research on Cancer (IARC) [35]. It is important to mention that welding leads to the formation of nanoparticles and iron represents about 80–95% wt% of welding fumes. However, co-exposure with known carcinogens, such as asbestos, chromium and nickel may be the most plausible explanation for the elevated cancer risk in welders.

Our study suggests adverse biological effects from inhalational occupational exposure to aerosol containing a high proportion of nano-sized iron oxide particles. This study supports our data from a pilot study where workers were exposed to nano-aerosol during titanium oxide (TiO₂) white pigment production. The results showed that markers of lipids, protein and nucleic acid oxidation were highly elevated ($p < 0.001$) in the EBC of workers both pre-shift and post-shift [36, 37]. It was also found that the elimination of TiO₂ particles from airways was rather slow, as they were still present in 40% of pre-shift EBC samples from workers, i.e. from the previous shift or shifts [38]. Also many experimental studies using TiO₂ particles document the biological effect of their nano form [39].

Iron oxides and TiO₂ both have low solubility and in the bulk form, they have a low systemic toxicity in humans. In nano iron oxide workers, oxidative stress markers in EBC were elevated; however, the total mass concentrations did not exceed the permissible exposure limit (PEL) for iron oxide particles, the occupational safety and health association (OSHA) limit for iron oxides fumes (10 mg m^{−3} time weighted average TWA concentration) [40] or the National Institute for Occupational Safety and Health (NIOSH) recommended exposure limit of 5 mg m^{−3} TWA [41]. The limits, however, have not been designed for iron nanoparticles.

Additionally, it should be mentioned, that oxidative stress and inflammation markers in EBC were elevated in patients previously exposed to carcinogenic inorganic dusts [29], silica [42] and asbestos [43] which can contain up to 30% iron [44].

Urinalysis of oxidative stress markers was also performed in this study to evaluate potential systemic

effects of iron oxide nanoparticles. The negative urinalysis results suggest there were likely no systemic effects.

Studies on the effects of environmental pollutants have been described by Gong [25, 26]. After the Beijing Olympics, it was found that gaseous pollutants, such as SO₂, were associated with elevated MDA and 8-OHdG levels in EBC and urine samples of inhabitants on the same day.

In our study, we did not find environmental air pollution to be an important factor because PM_{2.5} concentration, for instance, was about 10 × lower compared with the results from the study by Gong *et al* [26]. Still, two markers, 8-isoprostane and HNE showed an effect of O₃ and SO₂ in the multiple regression analysis; however it was not stronger than the effect of occupational exposure. Therefore, these markers do not appear to be the best predictors of the effect of nano Fe oxides.

One limitation of this study was the low number of subjects, due to a small number of workers in the factory. Even with this limitation, results in this study were still statistically significant at a 95% confidence interval. Another limitation was the fact that the chemical analysis of aerosol samples was not performed. Therefore, dust sediment samples were analysed by Raman microspectrometry to confirm the purity of the iron oxides dust.

5. Conclusions

To the best of our knowledge, this is the first study to examine oxidative stress markers in EBC and urine in workers exposed to nano iron oxides. The potential adverse effects of nanoparticles on human health are not well understood and research on this subject is a priority for the OECD, NIOSH and European Agency for Safety and Health at Work [45]. The importance of this type of research is high not only for the construction and coatings industries where iron oxide nanoparticles are produced in the process of pigment production, but also for industries that produce fertilizers, catalysts, magnetic materials, biomedical imaging materials and therapeutic agents.

Exposure to iron oxide nanoparticles has been extensively studied in rodents and results show that oxidative stress and inflammatory responses occur after exposure; however, no human studies have been conducted. The elevation of oxidative stress markers in EBC is in agreement with experimental data and with mechanisms of oxidative stress, based on epidemiological studies on major sources of carcinogenesis [46].

Based on our urinalysis results, iron oxide particle exposure did not result in systemic effects. However, this may be dependent on the level of iron oxide particle exposure.

The presence of lipid, nucleic acid and protein oxidation biomarkers in the EBC of workers expanded our understanding of the effect of nanoparticle inhalation in humans. To evaluate the elimination of iron oxide nanoparticles from the human body, we are

currently using Raman microspectroscopy and transition electron microscopy to further analyse EBC and urine samples.

Using the precautionary principle, all exposed employees, including research workers who are directly exposed to iron oxide nanoparticles should be monitored for potential side effects. EBC collection and analysis is a non-invasive method for monitoring effects of respiratory system nanoparticle exposure and should be evaluated in parallel with periodic physical examinations.

Conflict of interest

The authors claim no conflict of interests

Acknowledgments

The authors would like to thank to the Charles University in Prague project P 25/1LF/2, P28/1LF/6 and EU Project 'Material—Technical Research Base for the Diagnostics and Treatment of Environmentally-caused and Oncological Disorders and their Risks, in the General University Hospital in Prague' (reg. No. CZ.2.16/3.1.00/24.12).

References

- [1] OECD 2014 List of nanomaterials and physical-chemical endpoints addressed by the OECD testing programme Report on the OECD expert meeting on the physical chemical properties of manufactured nanomaterials and test guidelines Series on the safety of manufactured nanomaterials No 41 (www.oecd.org/officialdocuments/publicdisplaydocumentpdf/?cote=env/jm/mono%282014%2915&doclanguage=en)
- [2] Lewinski N, Graczyk H and Riediker M 2013 Human inhalation exposure to iron oxide particles *BioNanoMater.* **14** 5–23
- [3] Møller P and Loft S 2010 Oxidative damage to DNA and lipids as biomarkers of exposure to air pollution *Environ. Health Perspect.* **118** 1126–36
- [4] Hanini A, Schmitt A, Kacem K, Chau F, Ammar S and Gavard J 2011 Evaluation of iron oxide nanoparticle biocompatibility *Int. J. Nanomedicine* **6** 787–94
- [5] Kamel A H, Abdallah A M and El-Baradie H Y 1972 Effect of temperature on properties of calcined red iron oxide pigments *J. Appl. Chem. Biotechnol.* **22** 1209–15
- [6] Potter M J 2001 Iron oxide pigments *Annu. Rev. (Washington DC, U S Department of the Interior)* (http://minerals.usgs.gov/minerals/pubs/commodity/iron_oxide/750401.pdf)
- [7] Curwin B and Bertke S 2011 Exposure characterization of metal oxide nanoparticles in the workplace *J. Occup. Env. iron Hyg.* **8** 580–7
- [8] Kermanizadeh A, Balharry D, Wallin H, Loft S and Møller P. 2015 Nanomaterial translocation-the biokinetics, tissue accumulation, toxicity and fate of materials in secondary organs-a review *Crit Rev Toxicol.* **10** 837–72
- [9] Teeguarden J G *et al* 2014 Comparative iron oxide nanoparticle cellular dosimetry and response in mice by the inhalation and liquid cell culture exposure routes *Part. Fibre Toxicol.* **11** 46
- [10] Radu M, Munteanu M C, Petrache S, Serban A K, Dinu D, Hermenean A, Sima C and Dinischiotu A 2010 Depletion of intracellular glutathione and increased lipid peroxidation mediate cytotoxicity of hematite nanoparticles in MRC-5 cells *Acta Biochim. Pol.* **57** 355–60

- [11] Singh N, Jenkins G J, Asadi R and Doak S H 2010 Potential toxicity of superparamagnetic iron oxide nanoparticles (SPION) *Nano Rev.* **1** 5358
- [12] Singh N, Jenkins G J, Nelson B C, Marquis B J, Maffei T G, Brown A P, Williams P M, Wright C J and Doak S H 2012 The role of iron redox state in the genotoxicity of ultrafine superparamagnetic iron oxide nanoparticles *Biomaterials* **33** 163–70
- [13] Srinivas A, Rao P J, Selvam G, Goparaju A, Murthy P B and Reddy P N 2012 Oxidative stress and inflammatory responses of rat following acute inhalation exposure to iron oxide nanoparticles *Hum. Exp. Toxicol.* **31** 1113–31
- [14] Sotiriou G A I, Diaz E, Long M S, Godleski J, Brain J, Pratsinis S E and Demokritou P 2012 A novel platform for pulmonary and cardiovascular toxicological characterization of inhaled engineered nanomaterials *Nanotoxicology* **6** 680–90
- [15] Ma P, Luo Q, Chen J E, Gan Y P, Du J, Ding S M, Xi Z G and Yang X 2012 Intraperitoneal injection of magnetic Fe₃O₄—nanoparticle induces hepatic and renal tissue injury via oxidative stress in mice *Int. J. Nanomed.* **7** 4809–18
- [16] Bhattacharya K et al 2012 Comparison of micro- and nanoscale Fe⁺³-containing (Hematite) particles for their toxicological properties in human lung cells *in vitro Toxicol Sci.* **126** 173–82
- [17] Novotna B, Jendelova P, Kapcalova M, Rossner P Jr, Turnovcova K, Bagryantseva Y, Babic M, Horak D and Sykova E 2012 Oxidative damage to biological macromolecules in human bone marrow mesenchymal stromal cells labeled with various types of iron oxide nanoparticles *Toxicol Lett.* **210** 53–63
- [18] Syslova K, Bohmova A, Mikoska M, Kuzma M, Pelclova D and Kacer P 2014 Multimarker screening of oxidative stress in aging *Oxid. Med. Cell. Longev.* **2014** 562860
- [19] Møller P, Jacobsen N R, Folkmann J K, Danielsen P H, Mikkelsen L, Hemmingsen J G, Vesterdal L K, Forchhammer L, Wallin H and Loft S 2010 Role of oxidative damage in toxicity of particulates *Free Radic. Res.* **44** 1–46
- [20] Fuchs P, Loeseken C, Schubert J K and Miekisch W 2010 Breath gas aldehydes as biomarkers of lung cancer *Int. J. Cancer* **126** 2663–70
- [21] Møller P et al 2014 Oxidative stress and inflammation generated DNA damage by exposure to air pollution particles *Mutation Res. Rev. Mutation Res.* **762** 133–66
- [22] Raaschou-Nielsen O et al 2013 Air pollution and lung cancer incidence in 17 European cohorts: prospective analyses from the European study of cohorts for air pollution effects (ESCAPE) *Lancet Oncol.* **14** 813–22
- [23] Hamra G B et al 2014 Outdoor particulate matter exposure and lung cancer: a systematic review and meta-analysis *Environ. Health Perspect.* **122** 906–11
- [24] Beelen R et al 2015 Natural-cause mortality and long-term exposure to particle components: an analysis of 19 European cohorts within the multi-center ESCAPE project *Environ. Health Perspect.* **123** 525–33
- [25] Gong J et al 2013 Malondialdehyde in exhaled breath condensate and urine as a biomarker of air pollution induced oxidative stress *J. Exp. Sc. Environ. Epidemiol.* **23** 322–7
- [26] Gong J et al 2014 Comparisons of ultrafine and fine particles in their associations with biomarkers reflecting physiological pathways *Environ. Sci. Technol.* **48** 5264–73
- [27] Horvath I et al 2005 Exhaled breath condensate: methodological recommendations and unresolved questions *Eur. Resp. J.* **26** 523–48
- [28] Kuban P and Foret F 2013 Exhaled breath condensate: determination of non-volatile compounds and their potential for clinical diagnosis and monitoring *Anal. Chim. Acta* **805** 1–18
- [29] Syslova K, Kacer P, Kuzma M, Klusackova P, Fenclova Z, Lebedova J and Pelclova D 2008 Determination of 8-iso-prostaglandin F(2 α) in exhaled breath condensate using combination of immunoseparation and LC-ESI-MS/MS *J. Chromatogr. B Analyt. Technol. Biomed. Life Sci.* **867** 8–14
- [30] Syslova K, Kacer P, Kuzma M, Pankracova A, Fenclova Z, Vlckova S, Lebedova J and Pelclova D 2010 LC-ESI-MS/MS method for oxidative stress multimarker screening in the exhaled breath condensate of asbestosis/silicosis patients *J. Breath Res.* **4** 017104
- [31] Effros R M, Biller J, Foss B, Hoagland K, Dunning M B, Castillo D, Bosbous M, Sun F and Shaker R 2003 A simple method for estimating respiratory solute dilution in exhaled breath condensates *Am. J. Respir. Crit. Care Med.* **168** 1500–5
- [32] Vaughan J et al 2003 Exhaled breath condensate pH is a robust and reproducible assay of airway acidity *Eur. Respir. J.* **22** 889–94
- [33] Lykkesfeldt J 2007 Malondialdehyde as biomarker of oxidative damage to lipids caused by smoking *Clin. Chim. Acta* **380** 50–8
- [34] de Faria D L A, Venâncio Silva S and de Oliveira M T 1997 Raman microspectroscopy of some iron oxides and oxyhydroxides *J. Raman Spectrosc.* **28** 873–8
- [35] IARC 1990 Evaluation of carcinogenic risks to humans *Chromium, Nickel and Welding* vol 49 pp 448–525 (<http://monographs.iarc.fr/ENG/Monographs/vol49/mono49.pdf>)
- [36] Pelclova D et al 2012 Markers of oxidative stress are elevated in workers exposed to nanoparticles *Proc. of the 4th Int. Conf. on NANOCON (Brno, 23–25 October 2012)* (www.nanocon.eu/files/proceedings/04/reports/628.pdf)
- [37] Pelclova D et al 2015 Markers of oxidative damage of nucleic acids and proteins among workers exposed to TiO₂ (nano) particles *Occup. Environ. Med.* **73** 110–8
- [38] Pelclova D et al 2015 Raman microspectroscopy of exhaled breath condensate and urine in workers exposed to fine and nano TiO₂ particles: a cross-sectional study *J. Breath Res.* **9** 036008
- [39] Chang X H, Zhang Y, Tang M and Wang B 2013 Health effects of exposure to nano-TiO₂: a meta-analysis of experimental studies *Nanoscale Res. Lett.* **8** 1–10
- [40] OSHA 2015 Iron oxide fume (https://www.osha.gov/dts/chemicalsampling/data/CH_247400.html)
- [41] CDC 2015 Iron oxide dust and fume (as Fe) *NIOSH pocket guide to chemical hazard* Available from: (www.cdc.gov/niosh/npg/npgd0344.html)
- [42] Pelclova D, Fenclova Z, Kacer P, Kuzma M, Navratil T and Lebedova J 2007 8-isoprostane and leukotrienes in exhaled breath condensate in Czech subjects with silicosis *Ind. Health.* **45** 766–74
- [43] Pelclova D, Fenclova Z, Kacer P, Kuzma M, Navratil T and Lebedova J 2008 Increased 8-isoprostane, a marker of oxidative stress in exhaled breath condensate in subjects with asbestos exposure *Ind. Health.* **46** 484–9
- [44] Virta R L 2002 Asbestos: geology, mineralogy, mining, and uses (<http://pubs.usgs.gov/of/2002/of02-149/of02-149.pdf>)
- [45] EASHW 2014 Priorities for occupational safety and health research in Europe for the years 2013–2020 (Luxembourg: Publications Office of the European Union; European Agency for Safety and Health at Work) (<https://osha.europa.eu/en/publications/reports/summary-priorities-for-osh-research-in-eu-for-2013-20>)
- [46] Toyokuni S 2008 Molecular mechanisms of oxidative stress-induced carcinogenesis: from epidemiology to oxygenomics *IUBMB Life* **60** 441–7